Al-Azhar Engineering 16th International Conference

Vol. 19, No. 72, July 2024, 173 - 184

INVESTIGATION OF THE MODULUS OF ELASTICITY IN Al 7075/Al_2O_3 NANOCOMPOSITES USING PHASED ARRAY ULTRASONIC MEASUREMENTS

Mohamed Khaled*, Mazen Negm, Ramy Mohamed

Mechanical Engineering Department, Al-Azhar University-Cairo-Egypt

***Correspondence:** mohammadkhaled.18@azhar.edu.eg

Citation:

Mohamed Khaled, Mazen Negm and Ramy Mohamed," investigation of the modulus of elasticity in al 7075/al_2o_3 nanocomposites using phased array ultrasonic measurements ," Journal of Al-Azhar University Engineering Sector, vol. 19, pp. 173 - 184, 2024.

Received: 03 February 2024

Revised: 25 March 2024

Accepted: 07 April 2024

DOI: 10.21608/auej.2024.272262.1629

ABSTRACT

Elastic properties such as modulus of elasticity, shear modulus and Poisson ratio are important properties in some engineering applications. Determination of elastic modulus (e.g., by tension test, etc.) will destroy the material, and it is not useful for future purposes. We can also determine the elastic properties by nondestructive testing (NDT) without destroying the material. The aim of the present study is to evaluate the elastic constants (modulus of elasticity, shear modulus and Poisson ratio) of Al 7075 reinforced with 4, 8, and 10 wt.% of Al2O3 nanoparticles using phased array ultrasonic measurements. The semi-solid technique was used to prepare the Al7075/Al2O3 nanocomposite. A phased array ultrasonic apparatus was used to calculate the elastic properties in terms of the velocity of longitudinal and shear waves. The results showed that modulus of elasticity and shear modulus increased with increasing Al2O3 wt.%. The maximum modulus of elasticity and shear modulus attained in this study were 77.24 ± 0.53 GPa and 29.77 ± 0.22 GPa, for the Al 7075 with 10 wt. % of Al2O3, respectively. These results demonstrate the potential of using phased array ultrasonic measurements to calculate the elastic properties of Al 7075/Al2O3 nanocomposite.

KEYWORDS: Elastic modulus, Shear modulus, Poisson’s ratio and nondestructive testing

دراسة معامل المرونة في مركبات Al 7075/Al_2O_3 النانوية باستخدام قياسات الموجات فوق الصوتية المرحلية

محمد محمد خالد * ، مازن نجم ، رامى القاضى

قسم الهندسة الميكانيكية -كلية الهندسة- جامعة الأزهر بالقاهرة، مصر

***البريد الاليكتروني للباحث الرئيسي:** mohammadkhaled.18@azhar.edu.eg

الملخص العربي

تعتبر الخصائص المرنة مثل معامل المرونة ونسبة بواسون ومعامل القص من الخصائص المهمة في بعض التطبيقات الهندسية. سيؤدي تحديد معامل المرونة (على سبيل المثال، عن طريق اختبار التوتر، وما إلى ذلك) إلى تدمير المادة، ولن يكون مفيدًا للأغراض المستقبلية. يمكننا أيضًا تحديد الخصائص المرنة عن طريق الاختبار غير المدمر (NDT) دون تدمير المادة. الهدف من هذه الدراسة هو تقييم الثوابت المرنة (معامل المرونة، ونسبة بواسون، ومعامل القص) لـ Al 7075 المعززة بـ 4، 8، و 10٪ بالوزن من جسيمات Al_2O_3 النانوية باستخدام قياسات الموجات فوق الصوتية ذات المصفوفة المرحلية. تم استخدام التقنية شبه الصلبة لتحضير مصفوفة Al7075/Al_2O_3. تم استخدام جهاز الموجات فوق الصوتية ذو المصفوفة المرحلية لحساب الخواص المرنة بدلالة سرعة الموجات الطولية وموجات القص. أظهرت النتائج أن معامل المرونة ومعامل القص يزداد بزيادة وزن Al_2O_3. كان الحد الأقصى لمعامل المرونة ومعامل القص الذي تم تحقيقه هو 77.24 ± 0.53 GPa و 29.7 ± 0.22 GPa، على التوالي، للمركب Al 7075 بوزن 10 % من Al_2O_3. يمكن استخدام قياسات أجهزة الموجات

فوق الصوتية ذات المصفوفة المرحلية كتقنية NDT بنجاح لحساب بعض الخصائص المرنة مقارنة بنتائج الاختبار المدمرة من الدراسات السابقة.

الكلمات الدالة: معامل المرونة، معامل القص، نسبة بواسون و الاختبارات الغير إتلافية

1. INTRODUCTION

In contemporary times, nanocomposites have emerged as pivotal materials, driving technological progress and innovation across diverse industrial domains [1]. These substances are remarkably versatile in their uses, displaying enhanced mechanical and physical characteristics when contrasted with traditional single-component materials like metals, ceramics, and polymers, often employed as matrix materials [2,3]. Industries ranging from automotive to aerospace benefit from the expanded utility of composite materials, particularly in scenarios where mechanical robustness is paramount[4]. Nanocomposites demonstrate immense potential across various sectors, including energy storage, structural engineering, sensing technologies, and catalysis[5- 8]. Among these, metal matrix nanocomposites (MMNCs) occupy a prominent position in engineering applications, with aluminum and its alloys standing out as favored metal matrices due to their advantageous characteristics like low density and high strength [9-11]. Aluminum matrix nanocomposites (AMNCs) have become increasingly popular compared to traditional aluminum alloys due to their superior physical and mechanical properties, making them highly sought after in a wide range of industries. [4] Ceramic particulate-reinforced aluminum matrix composites (AMCs) offer a compelling blend of aluminum's ductility with the enhanced strength and toughness conferred by ceramic particles, making them ideal for weight-sensitive applications in automotive and aerospace sectors [3]. Leveraging aluminum-based composites to augment aluminum's performance as a promising anode material in lithium-ion batteries has yielded promising results. Significantly, aluminum nanocomposites like Al/MoS_2/C and Al/Fe/C demonstrate improved electrochemical behavior, increased stability, and extended cycle life in comparison to pure aluminum. [12,13]Ceramic particles, predominantly oxides or carbides, serve as the primary reinforcements in aluminum matrix composites (AMCs), with alumina (Al_2O_3) and silicon carbide (SiC) being the most prevalent choices. Alumina is notably utilized as a discontinuous reinforcement in Aluminum Matrix Composites (AMCs) to enhance compressive strength, hardness, and resistance to wear. [3, 4] The properties of ceramic particle-reinforced aluminum matrix composites (AMCs) are intricately linked to the alterations in microstructure resulting from the inclusion of ceramic particles and the adopted manufacturing methodology. Achieving uniform dispersion of these ceramic particles is pivotal in harnessing their small size and high strength effectively [14]. Understanding material microstructures and their associated mechanical traits is paramount for ensuring optimal material performance . Non-destructive evaluation (NDE) methods offer significant potential in evaluating microstructural variations, mechanical properties, texture, and thermo-mechanical characteristics of materials [15].Among NDE methods, ultrasonic testing (UT) stands out as a practical approach for assessing microstructural and mechanical properties across various material systems. By utilizing high-frequency sound waves, UT enables straightforward evaluation of materials that have undergone heat treatment, providing valuable insights into structural and microstructural variations[16-18]. Parameters such as ultrasonic velocity and attenuation offer crucial information about microstructure, grain size, porosity, stress state, and anisotropy in materials[19]. Furthermore, the use of ultrasonic characterization allows for the assessment of elastic constants, such as Young's modulus, shear modulus and bulk modulus. The velocity of acoustic waves is directly related to these constants and the density of the material. [20].In the context of AMCs, ultrasonic characterization holds particular intrigue for evaluating their properties. Research demonstrates the feasibility of indirectly assessing the microstructure and mechanical properties of AMCs through ultrasonic parameter measurements, with these parameters functionally associated with the structural and microstructural features of AMCs [21-23] Further exploration is essential to comprehensively understand the relationship between ultrasonic parameters and AMC microstructure. Motivated by these considerations, an experimental study was undertaken to investigate the applicability of ultrasonic pulse-echo techniques in characterizing Al 7075/Al_2O_3 nanocomposites . The nanocomposites were prepared using a semi-solid (compo casting) stir casting technique chosen for its precise control over microstructural parameters. The study aimed to establish correlations between the microstructural characteristics of Al 7075/Al_2O_3 nanocomposites —altered by varying Al_2O_3 content—and corresponding ultrasonic parameters.

2. EXPERIMENTAL WORK

2.1 MATERIALS

A commercially available aluminum alloy, Al 7075, was selected as the base material to be reinforced with alumina powder (Al_2O_3). The chemical composition of Al 7075 was attained by optical emission spectrometry (spark analysis) apparatus which located at Alumisr factory– Helwan city – Cairo- Egypt. Table 1 listed the chemical composition of Al 7075.

Table 1. Chemical composition of aluminum alloy 7075

Cr	Ti	Mn	Zn	Si	Cu	Fe	Mg	Other	Al	Alloy
0.18	0.07	0.17	5.35	0.42	1.2	0.62	2.3	0.15	Bal.	**7075**

The characterizations selected to identify the reinforced Al_2O_3 powder were scanning electron microscope (SEM), EDX and particle size distribution. **Fig. 1(A)** showed the SEM image of Al_2O_3 powder. It can be seen that Al_2O_3 powder has agglomerated and rod-like morphologies. However, the predominant particles morphology is those with rod-like one. The purity of the Al_2O_3 powder used was tested by EDX . **Fig. 1(B)** showed the EDX results that confirmed the exceptional purity of the Al_2O_3 powder. The specific particle size plays a crucial role, influencing how these particles disperse and interact within the matrix, ultimately shaping the material's overall properties. In the current experiment, the average particle size distribution peak of Al_2O_3 powder was 0.69 ± 0.07 µm; **Fig. 2**. The examination was carried out at the Faculty of Science, Al-Azhar University, Cairo, Egypt.

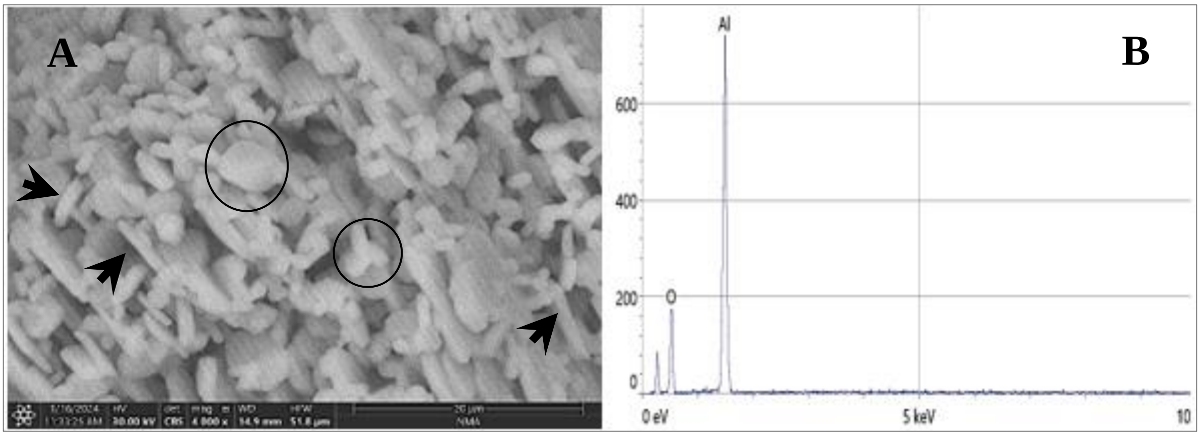

Fig. 1: A) SEM image of Al_2O_3 powder. Arrows and circles are pointed to rods like and agglomerated particles respectively. **B)** EDX result of Al_2O_3 powder

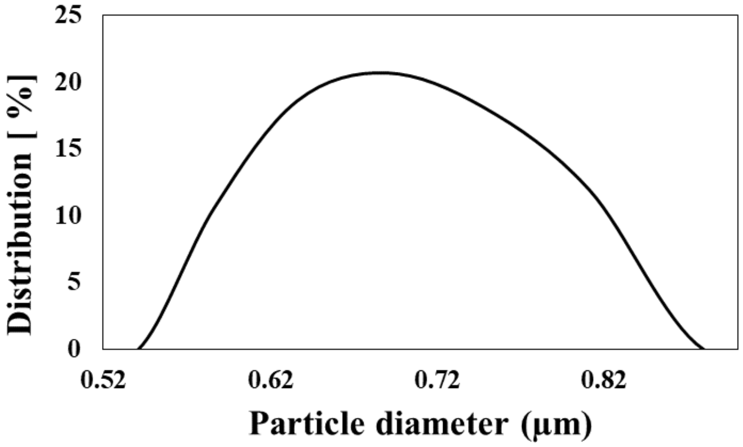

Fig. 2. Particle size distribution of Al_2O_3 powder

To enhance the mechanical characteristics of the base alloy (Al 7075) , we intentionally introduced varying quantities of Al_2O_3 powder — specifically 4 wt.%, 8 wt.%, and 10 wt.%. These different percentages of Al_2O_3 powder were added to the Al 7075 base alloy using Semi solid technique (compo casting). The process begins with 400 grams of Al 7075 alloy being melted in a crucible, gradually heated in a heat-resistant furnace until it reaches 750 °C, and maintained at this temperature for one hour. Additionally, hexachloroethane powder is introduced to the molten Al 7075 to effectively remove slag. The melted Al 7075 is then intentionally cooled below the liquid state to maintain a semi-solid slurry. To improve wettability, Al_2O_3 powder are preheated at 500°C for three hours. Automatic stirring is accomplished using a radial stirrer driven by an electric DC motor, operating for approximately 3 to 4 minutes at a stirring rate of 350 revolutions per minute (rpm).During this stage, the preheated Al_2O_3 powder are manually introduced into the molten. Throughout the final mixing stages, temperature control is carefully maintained within the range of 550 ± 10°C. After the process is completed, the molten composite undergoes a temperature increase to 750 ± 10°C following the stirring process. Subsequently, the molten composite is poured into a mold measuring 200 mm x 100 mm x 8 mm, which has been preheated to 350 ± 10°C, shaping the specimen as desired.

2.2 CHARACTERIZATION

2.2.1 DENSITY MEASUREMENTS

The density of the samples was determined experimentally through Archimedes' principle. This technique calculates the buoyant force on a submerged object, equivalent to the weight of the fluid that the object displaces. The examination was carried out at mechanical engineering department - faculty of engineering , Al-Azhar University, - Cairo, Egypt. The density (ρ) of specimens in this study were calculated using equation (1) :

$$\rho = \frac{m\,(Kg)}{V(m^3)} \qquad (1)$$

2.2.2 MORPHOLOGIC AL ANALYSIS

Specific specimens were subjected to scanning electron microscope (SEM) analysis using a QUANTA FEG 250 model, which operates at 150.00 kV and is equipped with an LFD detector. This instrument is located at the Faculty of Science, Banha University, Banha, Egypt. To reveal the microstructure, the specimens underwent etching using a solution composed of 1.5 vol.% concentrated HF, 2.5 vol.% concentrated NHO_3, and vol.% HCl in 95 vol.% distilled water.

2.2.3 ULTRASONIC MEASUREMENTS

Prior to commencing the ultrasonic measurements, thorough consideration was given to designing the geometry and dimensions of the specimens to mitigate any potential sidewall effects. The nan composite specimens were meticulously polished to achieve smooth, flat, and parallel surfaces. The parallelism between opposite faces was confirmed using a surface plate with an accuracy of ±2 mm. Ultrasonic testing was conducted using a commercially available phased array apparatus which consists of an ultrasonic oscilloscope (Agilent, 100 MHz), an ultrasonic pulsar/receiver (Olympus, USA), and transducers (Olympus, USA). The phased array apparatus used located at GAC company-Nasr city- Cairo- Egypt. The transducers are an essential components of the setup, comprising both straight normal and angle beam transducers. In particular, straight-beam transducers with 16 crystals operating at 5 MHz (Olympus SA10-5 L16) were used for generating longitudinal waves, while an angle beam transducer with a frequency of 5 MHz was employed to generate shear waves. Ultrasonic measurements were conducted using the direct contact method between the transducer and specimens in a pulse-echo configuration. The employed software enabled real-time signal acquisition and velocity determination. The schematic drawing of setup of the phased array method for velocities measurement are illustrated in **Fig. 3(A)**. To determine the longitudinal wave velocity (V_l) and shear wave velocity (V_s), two consecutive back-wall echoes were captured from the oscilloscope. The accurate time delay between these echoes was measured employing a cross-correlation technique combined with an interpolation method. Subsequently, velocities were computed from the time delay or time of flight (TOF) between the two consecutive back-wall echoes and the thickness of the specimen, **Fig. 3(B)**, utilizing the equation (2) [21]:

$$\boldsymbol{Velocity} = \frac{\mathbf{2} * \boldsymbol{thickness}\ (\boldsymbol{m})}{\boldsymbol{time}\ (\boldsymbol{s})} \qquad (2)$$

In equation (2), the factor of 2 accounts for the adjustment in the ultrasonic wave's travel distance due to the use of a pulse-echo configuration. Specifically, the 2nd and 3rd back-wall echoes were chosen for measurements to minimize interference phenomena linked with the nearfield [14]. Velocity is denoted in meters per second (m/s). To ensure precision, the average of three measurements from five distinct signal acquisitions was computed, and the mean value was recorded. The absolute accuracy in velocity measurement was ±10%.

Fig. 3 A) schematic drawing of phased array method as the waves pass through the specimen and return to the transducer [24]. **B**) Interface screen of phased array apparatus, the horizontal axis typically represents distance, while the vertical axis represents the amplitude or intensity of the ultrasonic wave.

3. RESULTS

3.1 VELOCITY MEASUREMENTS

The examination was carried out on aluminum alloy 7075, incorporating various Al_2O_3 proportions: 0%, 4%, 8%, and 10%. The findings were documented in **Table 2.** Each proportion underwent testing with three distinct specimens, and five velocity measurements were recorded for each specimen. **Table 2** presents the calculated and observed values of ultrasonic longitudinal wave velocity (V_l) and shear wave velocity (V_s) relative to the Al_2O_3 percentages. Significantly, both the longitudinal wave velocity (V_l) and shear wave velocity (V_s) values demonstrated an increase with the increasing of Al_2O_3 percentages.

Table 2 The actual values obtained for longitudinal and shear-phased array ultrasonic velocities by 5 MHz transducers for each respective specimen in Al 7075/Al_2O_3 nanocomposites .

Al_2O_3 (wt. %)	Longitudinal Velocity **V_l**	Shear Velocity **V_s**
0	6027.0 ± 24.12	3090.6 ± 8.20
4	6156.8 ± 15.35	3186.2 ± 9.9
8	6254.8 ± 11.82	3359 ± 13.84
10	6424.6 ± 26.33	3450.8 ± 12.7

3.2 ELASTIC CONSTANTS

The elastic properties of Al 7075/Al_2O_3 were assessed using acoustic velocity elasticity relationships. The elastic constants of the specimens, comprising shear modulus (G), modulus of elasticity (E), and Poisson's ratio (ν), were calculated based on the measured ultrasonic longitudinal and shear wave velocities, as well as density, adhering to ASTM E 494-2005 [25]. The elastic constants, represented by G, E, and ν, were determined computationally utilizing the relationship between longitudinal and shear ultrasonic velocities, as described by Equations 3, 4, and 5, provided that the density is known. In the current study, the density was determined using Archimedes' theory, yielding values of 2.54 ± 0.0, 2.57 ± 0.009, 2.61 ± 0.011, and 2.72 ± 0.013 g/cm^3 for Al 7075 reinforced with 0%, 4%, 8%, and 10% Al_2O_3, respectively. Density results showed a fluctuation that is not significant, implying that density is not the primary variable affecting ultrasonic velocity .The numerically calculated elastic constants of Al 7075/Al_2O_3 nanocomposites are presented in **Table 3**. Notably, elastic constants exhibit an approximately linear increase with the augmentation of Al_2O_3 percentages. Intriguingly, the observed trends of elastic constants mirror those of ultrasonic velocities, with each modulus of G, E, and ν following a similar pattern. In Al7075/Al_2O_3 nanocomposites , the variation in elastic modulus between the malleable Al matrix and the more rigid Al_2O_3 nanoparticles results in an elevation of both V_l and V_s velocities. Furthermore, the augmentation of Al_2O_3 content enhances the Young's modulus of Al 7075/Al_2O_3 nanocomposites [14], leading to an increase in both V_l and Vs velocities.

Shear modulus $$\mathbf{G} = \rho \mathrm{V}_s{}^2 \tag{3}$$

Modulus of elastesity $$\mathbf{E} = \frac{\rho \mathrm{V}_s{}^2(3\mathrm{V}_l{}^2-4\mathrm{V}_s{}^2)}{\mathrm{V}_l{}^2-\mathrm{V}_s{}^2} \tag{4}$$

Poisson`s ratio $$\upsilon = \frac{(V_l^2 - 2V_s^2)}{2(V_l^2 - V_s^2)} \qquad (5)$$

Table 3 displays the elastic properties of Al 7075/Al_2O_3 nanocomposites in relation to the Al_2O_3 content, as determined using 5 MHz transducers.

Al_2O_3 (wt.%)	**E** (GPa)	**G** (GPa)	**Poisson' ratio (υ)**
0	62.99 ± 0.25	23.88 ± 0.13	0.32 ± 0.003
4	66.85 ± 0.33	25.25 ± 0.4	0.32 ± 0.005
8	73.18 ± 0.467	28.20 ± 0.23	0.30 ± 0.003
10	77.24 ± 0.53	29.77 ± 0.22	0.30 ± 0.002

4. DISCUSSION

4.1 VELOCITY MEASUREMENTS

As previously noted, the incorporation of Al_2O_3 nanoparticles significantly affects both longitudinal (V_l) and shear (V_s) velocities. Table 2 illustrates a notable increase in V_l and V_s velocities in the presence of dispersed Al_2O_3 compared to pure Al 7075. Consequently, the addition of Al_2O_3 nanoparticles results in a stiffer matrix compared to pure Al 7075, leading to higher V_l and V_s velocities. The ultrasonic wave propagates faster within the stiffer phase (Al_2O_3) compared to the base metal matrix. The elevation in these velocities aligns with anticipations, attributing to the reinforced matrix's increased rigidity with the incorporation of higher Al_2O_3 nanoparticle concentrations.

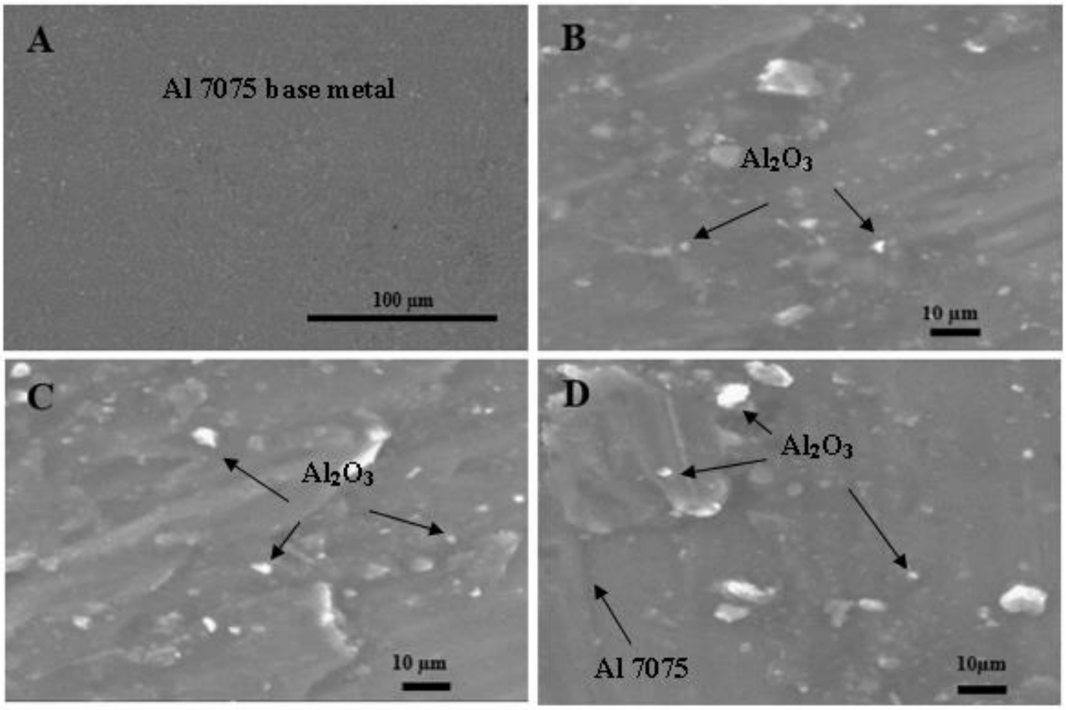

Fig. 4 SEM images of Al 7075 base metal with Al2O3 percentage equal to A) 0 wt. %, B) 4 wt. % C) 8 wt. % D) 10 wt. %

Fig. 4 showed dispersion of Al_2O_3 nanoparticles within the Al 7075 matrix with 0, 4, 8 and 10 wt. %. The values of V_l and Vs velocities in Al 7075/Al_2O_3 nanocomposites increase with the increasing of Al_2O_3 content, consistent with the expected trend due to the stiffer matrix with higher Al_2O_3 content. Similar observations were recorded by Gür & Ogel [19], Collins & Alcheikh [26] . They prepared Al/SiC nanocomposites and reported that ultrasonic velocities increased as the reinforcement content of SiC increased [19,25].

Fig.5 showed the relationship between Al_2O_3 wt. % versus longitudinal (V_l) and shear velocities (V_s). It can be seen that both V_l and V_s exhibit a nearly linear relationship with the escalating Al_2O_3 content, indicating that E can be reliably predicted by measuring V_l and V_s. In Al 7075/Al_2O_3 nanocomposites, the density fluctuation is minimal, suggesting that density is not a primary variable influencing ultrasonic velocity. Regarding ultrasonic wave frequency, it has no significant effect on the velocities of ultrasonic waves. [2]

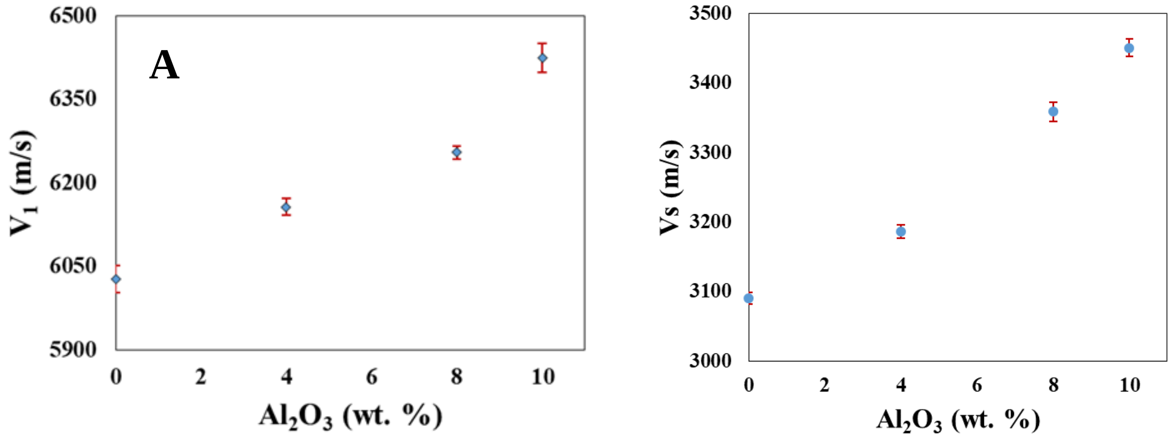

Fig.5 A) shear velocity and **B)** longitudinal velocity of the phased array ultrasound waves passed through Al7075 reinforced with 0, 4, 8 and 10 wt. % of Al_2O_3

4.2 ELASTIC CONSTANTS

Table 3 reveals a correlation between the elastic constants, Specifically E and G values, and ultrasonic velocities. The E and G values showed a direct correlation with the rising percentage of Al_2O_3; **Fig.6 (B).** Enhanced E values in these nanocomposites suggest a strong interfacial adhesion between the Al matrix and Al_2O_3 nanoparticles, which is attributed to the uniform dispersion and reduced spacing between Al_2O_3 particles. The even distribution of Al_2O_3 nanoparticles improves the transfer of load from the matrix to the reinforcing material, leading to increased E values [21]. Furthermore, it has been observed that Poisson's ratio (ν) remains relatively stable amidst shifts in the elastic constants. The predicted ν values imply the presence of ionic contributions in all Al 7075/Al_2O_3 nanocomposites. Hence, to enhance the modulus of elasticity values, there is a concurrent decrease in ductility with the increasing alumina content. This trend suggests a trade-off between the mechanical properties of the composite material, wherein the reinforcement with alumina leads to improved stiffness at the expense of reduced ductility. Additionally, the escalating values of G ; **Fig.6 (A),** indicate a more pronounced directional bonding between atoms. In this study, the modulus of elasticity of Al 7075 reinforced with 0 and 4 wt.% of Al_2O_3 was equal to 62.99 ± 0.25 and 66.85 ± 0.33GPa respectively. These results are almost in line with the experimental study (tension test) that recorded the modulus of elasticity (E) of Al 7075 reinforced with 0 and 5 wt.% of Al_2O_3 was equal to 70.6 and 80.29 GPa, respectively [26]. The main finding in this study demonstrate the potential of using phased array ultrasonic measurements to calculate the elastic properties of Al 7075/Al_2O_3 nanocomposite instead of the traditional tension test. Elastic properties are the main parameters required in finite element software to evaluate the mechanical design of the part /system responded in an elastic way.

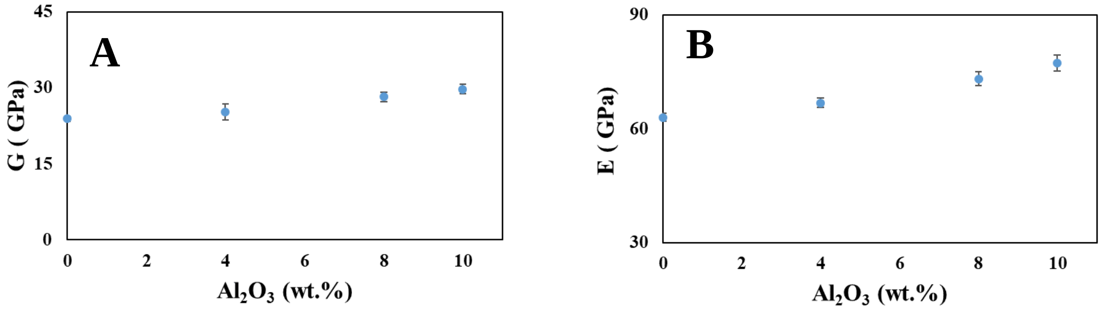

Fig.6 A) shear modulus and **B)** modulus of elasticity of Al7075 reinforced with 0, 4, 8 and 10 wt. % of Al_2O_3 calculated from the equations of longitudinal and shear velocities of phased array ultrasound waves

CONCLUSIONS

The changes in ultrasonic velocities have been linked to the microstructural characteristics of the Al 7075/Al_2O_3 nanocomposites. These characteristics encompass the concentration of Al_2O_3, and the uniform dispersion of Al_2O_3 nanoparticles. From these observations, several key conclusions are summarized:

1. As the percentage of Al_2O_3 increases, along with its even distribution and refinement within the composite, there is a consistent increase in the velocities of both longitudinal (V_l) and shear (V_s) waves. The primary reason behind the rise in Vl and Vs velocities is the enhancement of the elastic modulus in the Al 7075/Al_2O_3 nanocomposites. Furthermore, the relationship between V_l and V_s velocities and the elastic modulus (E) values is observed to be approximately linear.
2. The pattern witnessed in the elastic constants corresponds to that observed in ultrasonic velocities, suggesting a rise in their values in tandem with the increase in Al_2O_3 content. The substantial increase in the modulus of elasticity (E) with the incorporation of Al_2O_3 highlights the significant influence of Al_2O_3 content on the material's stiffness and overall mechanical characteristics.
3. The present study highlights the sensitivity of the material's elastic modulus to minor compositional changes resulting from the formation of intermetallic phases on the additive Al_2O_3 (4%, 8%, and 10%), which can be effectively monitored by ultrasonic techniques From the present study, it is evident that the elastic modulus of the material are very sensitive to any

minor compositional changes resulting from the formation of intermetallic phases on the additive Al_2O_3 (4%, 8%, and 10%) and can be effectively monitored by ultrasonic.

References s

[1] R. A. M. Said, M. A. Hasan, A. M. Abdelzaher, and A. M. Abdel-Raoof, “Review—Insights into the Developments of Nanocomposites for Its Processing and Application as Sensing Materials,” J Electrochem Soc, vol. 167, no. 3, p. 037549, Jan. 2020, doi: 10.1149/1945-7111/ab697b.

[2] M. Toozandehjani, K. A. Matori, F. Ostovan, K. R. Jamaludin, A. Amrin, and E. Shafiei, “The Effect of the Addition of CNTs on the Microstructure, Densification and Mechanical Behavior in Al-CNT-Al_2O_3 Hybrid Nanocomposites,” JOM, vol. 72, no. 6, pp. 2283–2294, Jun. 2020, doi: 10.1007/s11837-020-04132-5.

[3] M. TOOZANDEHJANI, F. OSTOVAN, K. R. JAMALUDIN, A. AMRIN, K. A. MATORI, and E. SHAFIEI, “Process microstructure properties relationship in Al−CNTs−Al_2O_3 nanocomposites manufactured by hybrid powder metallurgy and microwave sintering process,” Transactions of Nonferrous Metals Society of China, vol. 30, no. 9, pp. 2339–2354, Sep. 2020, doi: 10.1016/S1003-6326(20)65383-3.

[4] P. Garg, A. Jamwal, D. Kumar, K. K. Sadasivuni, C. M. Hussain, and P. Gupta, “Advance research progresses in aluminium matrix composites: manufacturing & applications,” Journal of Materials Research and Technology, vol. 8, no. 5, pp. 4924–4939, Sep. 2019, doi: 10.1016/j.jmrt.2019.06.028.

[5] Z. Tan, J. Li, and Z. Zhang, “Experimental and numerical studies on fabrication of nanoparticle reinforced aluminum matrix composites by friction stir additive manufacturing,” Journal of Materials Research and Technology, vol. 12, pp. 1898–1912, May 2021, doi: 10.1016/j.jmrt.2021.04.004.

[6] Q. Shi et al., “A review of recent developments in Si/C composite materials for Li-ion batteries,” Energy Storage Mater, vol. 34, pp. 735–754, Jan. 2021, doi: 10.1016/j.ensm.2020.10.026.

[7] J. C. de Haro et al., “Lignin-Based Polymer Electrolyte Membranes for Sustainable Aqueous Dye-Sensitized Solar Cells,” ACS Sustain Chem Eng, vol. 9, no. 25, pp. 8550–8560, Jun. 2021, doi: 10.1021/acssuschemeng.1c01882.

[8] T. E. Glier et al., “Conductance-strain behavior in silver-nanowire composites: network properties of a tunable strain sensor,” Nanotechnology, vol. 32, no. 36, p. 365701, Sep. 2021, doi: 10.1088/1361-6528/ac04a4.

[9] V. Chak, H. Chattopadhyay, and T. L. Dora, “A review on fabrication methods, reinforcements and mechanical properties of aluminum matrix composites,” J Manuf Process, vol. 56, pp. 1059–1074, Aug. 2020, doi: 10.1016/j.jmapro.2020.05.042.

[10] M. Imran and A. R. A. Khan, “Characterization of Al-7075 metal matrix composites: a review,” Journal of Materials Research and Technology, vol. 8, no. 3, pp. 3347–3356, May 2019, doi: 10.1016/j.jmrt.2017.10.012.

[11] Z. Chen, J. Qian, X. Ai, Y. Cao, and H. Yang, “Electrochemical performances of Al-based composites as anode materials for Li-ion batteries,” Electrochim Acta, vol. 54, no. 16, pp. 4118–4122, Jun. 2009, doi: 10.1016/j.electacta.2009.02.049.

[12] C. Suryanarayana and N. Al-Aqeeli, “Mechanically alloyed nanocomposites,” Prog Mater Sci, vol. 58, no. 4, pp. 383–502, May 2013, doi: 10.1016/j.pmatsci.2012.10.001.

[13] M. Toozandehjani, K. A. Matori, F. Ostovan, F. Mustapha, N. I. Zahari, and A. Oskoueian, “On the correlation between microstructural evolution and ultrasonic properties: a review,” J Mater Sci, vol. 50, no. 7, pp. 2643–2665, Apr. 2015, doi: 10.1007/s10853-015-8855-x.

[14] M. Toozandehjani et al., “Characterization of Aging Behavior of AA6061 Aluminum Alloy Through Destructive and Ultrasonic Non-destructive Testing Techniques,” Transactions of the Indian Institute of Metals, vol. 68, no. 4, pp. 561–569, Aug. 2015, doi: 10.1007/s12666-014-0486-4.

[15] Y. Song, X. Zi, Y. Fu, X. Li, C. Chen, and K. Zhou, “Nondestructive testing of additively manufactured material based on ultrasonic scattering measurement,” Measurement, vol. 118, pp. 105–112, Mar. 2018, doi: 10.1016/j.measurement.2018.01.020.

[16] E. Seixas, G. R. Pereira, J. M. A. Rebello, C. S. Velloso, and C. A. Costa, “Applicability of nondestructive testing to detect cavities in PVDF polymer,” Journal of Materials Research and Technology, vol. 9, no. 6, pp. 13294–13300, Nov. 2020, doi: 10.1016/j.jmrt.2020.09.069.

[17] T. Sol, S. Hayun, D. Noiman, E. Tiferet, O. Yeheskel, and O. Tevet, “Nondestructive ultrasonic evaluation of additively manufactured AlSi10Mg samples,” Addit Manuf, vol. 22, pp. 700–707, Aug. 2018, doi: 10.1016/j.addma.2018.06.016.

[18] H. Wu, M. Zhao, C. Chang, and Q. Lu, “The Real Culprit in Systemic Lupus Erythematosus: Abnormal Epigenetic Regulation,” Int J Mol Sci, vol. 16, no. 12, pp. 11013–11033, May 2015, doi: 10.3390/ijms160511013.

[19] C. H. Gür and B. Ogel, “Non-destructive microstructural characterization of aluminium matrix composites by ultrasonic techniques,” Mater Charact, vol. 47, no. 3–4, pp. 227–233, Sep. 2001, doi: 10.1016/S1044-5803(01)00174-7.

[20] A. A. El-Daly, M. Abdelhameed, M. Hashish, and W. M. Daoush, “Fabrication of silicon carbide reinforced aluminum matrix nanocomposites and characterization of its mechanical properties using non-destructive technique,” Materials Science and Engineering: A, vol. 559, pp. 384–393, Jan. 2013, doi: 10.1016/j.msea.2012.08.114.

[21] A. A. El-Daly, M. Abdelhameed, M. Hashish, and A. M. Eid, “Synthesis of Al/SiC nanocomposite and evaluation of its mechanical properties using pulse echo overlap method,” J Alloys Compd, vol. 542, pp. 51–58, Nov. 2012, doi: 10.1016/j.jallcom.2012.07.102.

[22] A. A. El-Daly, F. El-Tantawy, A. E. Hammad, M. S. Gaafar, E. H. El-Mossalamy, and A. A. Al-Ghamdi, “Structural and elastic properties of eutectic Sn–Cu lead-free solder alloy containing small amount of Ag and In,” J Alloys Compd, vol. 509, no. 26, pp. 7238–7246, Jun. 2011, doi: 10.1016/j.jallcom.2011.01.062.

[23] A. A. El-Daly and A. E. Hammad, “Elastic properties and thermal behavior of Sn–Zn based lead-free solder alloys,” J Alloys Compd, vol. 505, no. 2, pp. 793–800, Sep. 2010, doi: 10.1016/j.jallcom.2010.06.142.

[24] M. Toozandehjani, F. Ostovan, M. Shamshirsaz, K. A. Matori, and E. Shafiei, “Velocity and attenuation of ultrasonic wave in Al–Al_2O_3 nanocomposite and their correlation to microstructural evolution during synthesizing procedure,” Journal of Materials Research and Technology, vol. 15, pp. 2529–2542, Nov. 2021, doi: 10.1016/j.jmrt.2021.09.065.

[25] “ASTM E494-05. Standard practice for measuring ultrasonic velocity in materials. West Conshohocken, PA: ASTM”.

[26] D. N. Collins and W. Alcheikh, “Ultrasonic non-destructive evaluation of the matrix structure and the graphite shape in cast iron,” J Mater Process Technol, vol. 55, no. 2, pp. 85–90, Nov. 1995, doi: 10.1016/0924-0136(95)01789-5.

[27] M. S. H. Al-Furjan, M. H. Hajmohammad, X. Shen, D. K. Rajak, and R. Kolahchi, “Evaluation of tensile strength and elastic modulus of 7075-T6 aluminum alloy by adding SiC reinforcing particles using vortex casting method,” J Alloys Compd, vol. 886, p. 161261, Dec. 2021, doi: 10.1016/j.jallcom.2021.161261.